

A STATIC AND DYNAMIC NONLINEAR BEHAVIOUR OF STEEL TOWERS OF LONG-SPAN SUSPENSION BRIDGES SUBJECT TO WIND AND EARTHQUAKE LOADINGS

By Taweep CHAISOMPHOB, Akio HASEGAWA** and Fumio NISHINO****

The static ultimate strength analyses of the tower-cable system of Akashi-Kaikyo Bridge are performed for the investigations of the planar and spatial behaviour of the structures subject to a variety of the combinations of the vertical dead and live loads, and the horizontal wind loads both in the directions of perpendicular-to-bridge axis and bridge axis. The obtained ultimate loads based on three different loading paths are compared with the design loads specified in the current codes of huge towers. The nonlinear dynamic responses of the planar tower and tower-cable models are obtained to examine the safety of the superstructures of Akashi towers against horizontal ground motions of the 1940 El Centro record with variable amplitudes up to four times the design acceleration specified in the codes.

Keywords : suspension bridge, tower, cable, ultimate strength, wind, nonlinear dynamic, earthquake

1. INTRODUCTION

Among the main components of long-span suspension bridges, the main towers together with the main cables may be regarded as the most important components due to the fact that the failure of any of the main towers may cause the sudden overall collapse of the suspension bridge system, while the bridge may survive despite the damage of hanger cables or part of girders. In the current design practice of the towers¹⁾, the design procedures seem to be too simplified for such a huge and important structure. For example, the design analyses are performed separately in the planes of perpendicular-to-bridge axis and bridge axis, and the members are designed by the column strength formula with vague boundary and loading conditions¹⁾. An incompleteness of such design recommendation may be due to the lack of investigations on the exact behaviour of the towers under a wide variety of design loadings.

This paper presents the nonlinear static and dynamic analyses of the main towers of the Akashi-Kaikyo Bridge subject to the combinations of the dead and live loads, the wind loads, and the earthquake loads. The bridge which is one of the Honshu-Shikoku Bridge Projects is now under the first stage of construction for its seabed^{2),3)}. It is noted that the present paper is extended from the previous paper³⁾ which has dealt with the nonlinear static analysis only for the case of vertical dead and live loads. The planar and spatial tower-cable models and the analytical procedures for the tower-cable system which have been developed in Ref. 3) are utilized in the present analysis. The static inelastic finite displacement analysis³⁾ is performed to obtain the load-displacement curves of the planar and spatial models subject to a variety of the combinations of the vertical dead and live loads, and the horizontal wind loads in the directions both of

* Dr. Eng., Ohbayashi Corporation Co. Ltd. (2-12-5, Uchikanda, Chiyoda-Ku, Tokyo 113), formerly Graduate Student, Department of Civil Engineering, University of Tokyo.

** Member of JSCE, Dr. Eng., Professor, Department of Civil Engineering, University of Tokyo (Bunkyo-ku Tokyo 113).

*** Member of JSCE, Ph.D., Professor, Department of Civil Engineering, University of Tokyo (Bunkyo-ku Tokyo 113).

perpendicular-to-bridge axis and bridge axis according to three representative loading paths defined as : I) varying vertical loads only, II) varying horizontal loads only, and III) varying both vertical and horizontal loads proportionally.

Based on the Newmark time integration ($\beta=1/4$) and one-step Newton-Raphson iteration, the incremental equation of motion is formulated to incorporate the effects of the structural consistent mass, the structural damping using the method of modal damping ratios, the material hysteresis, and the soil-interaction using the linear spring models of pier structures. By performing a step-by-step time integration, the nonlinear dynamic responses of the planar tower and tower-cable models under the application of the constant design vertical dead and live loads, and the horizontal ground motions of the 1940 El Centro accelerogram with variable amplitudes in both directions are obtained for the 30-second time history.

From the present numerical results, the ultimate loads obtained by adopting the above loading paths of the combinations of the dead and live loads, and the wind loads are compared with the design loads specified in the current codes of the towers¹⁾. In addition, the safety of the superstructures of towers against rather strong earthquake loads of four times the specified design acceleration⁴⁾ is examined.

2. METHOD OF ANALYSIS

Since the analytical procedure proposed in Ref. 3) is applicable to the analysis of the tower-cable system of suspension bridges regardless of loading conditions, it is adopted for the present static analysis of the planar and spatial tower-cable models subject to the combinations of the vertical dead and live loads, and the horizontal wind loads. It is noted that, because of sufficient flexibility of hangers, the stiffening girder is treated simply as dead and wind loads for the tower-cable system, and hence the interaction between the stiffening girder and the tower-cable system is not considered at present static analysis. In the case of the dynamic analysis due to the horizontal ground motions, the following modifications are needed.

(1) Step-by-step time integration analysis

By adding the inertia and damping terms to the incremental stiffness equation derived in Ref. 3), the incremental equation of motion at time step $(n+1)$, $t = t^n + \Delta t = t^{n+1}$ (Δt is the size of time step) can be written as⁵⁾

$$K^n \Delta u^n + M \dot{u}^{n+1} + C \ddot{u}^{n+1} = F^{n+1} - P^n \dots\dots\dots (1)$$

where

$$\Delta u^n = u^{n+1} - u^n \dots\dots\dots (2)$$

in which K is the tangential stiffness matrix ; u and F are the vectors of nodal displacement and external forces, respectively ; P is the vector of nodal point forces equivalent to the element stresses⁵⁾; M and C are the structural mass and damping matrices, respectively ; the differentiation with respect to time is indicated by a dot, ($\dot{}$), and hence, \dot{u} and \ddot{u} are the vectors of nodal velocity and acceleration. Substituting the expression of \dot{u}^{n+1} and \ddot{u}^{n+1} based on the Newmark time integration with the value of $\beta=1/4$ into Eq. (1) yields⁵⁾.

$$\left\{ K^n + \frac{2}{\Delta t} C + \frac{4}{\Delta t^2} M \right\} \Delta u^n = F^{n+1} - P^n + C \dot{u}^n + M \left(\frac{4}{\Delta t} \dot{u}^n + \ddot{u}^n \right) \dots\dots\dots (3)$$

By solving Eq. (3) for incremental displacement Δu^n , the unknown variables at t^{n+1} , i. e., u^{n+1} , \dot{u}^{n+1} and \ddot{u}^{n+1} corresponding to the given external force F^{n+1} can be obtained. It is noted that this procedure does not involve the equilibrium iteration during each time step. In other words, Eq. (3) is equivalent to one-step iteration of Newton-Raphson procedure for the loading control technique. The cumulative errors due to this one-step iteration may be reduced by shortening the size of time step Δt . By varying time steps to be 0.005, 0.01, 0.02 second, respectively, and obtaining the responses of 30-second time history using each of three different time steps, it is found that a difference among those three results is less than 5 %, and hence the time step 0.02 second is employed throughout this analysis.

(2) Externally applied earthquake loads

In most cases⁶⁾, the external force due to ground motions for the single-degree-of freedom (SDOF) system is represented by the effective force equal to the product between structural mass and ground acceleration. For the sake of simplicity, by assuming that the earthquake ground acceleration produces the same acceleration for all points of structural system, the same concept as in SDOF system is applied to the present problem of multi-degree-of-freedom system. The external force vector F^{n+1} in Eq. (3) is, therefore, expressed by

$$F^{n+1} = M r \ddot{u}_g^{n+1} \dots\dots\dots (4)$$

where \ddot{u}_g^{n+1} denotes the horizontally translational acceleration of ground and r is the vector containing unit value for the components corresponding to the horizontal translation and zero for the rest. It is noted that by adopting Eq. (4), u , \dot{u} , and \ddot{u} are the relative quantities with respect to horizontal ground motions.

(3) Structural properties

As in case of static analyses, the material model using average stress-strain relation described in Ref. 3) is adopted for towers and the linear elastic material is adopted for cables. To account for the hysteresis of materials, the simplest model which considers elastic unloading only but neglects the Bauschinger and strain hardening effects is introduced. As can be seen later in numerical dynamic results which are concerned only within an elastic range, the influences of Bauschinger and strain hardening are ineffective.

For the mass properties of tower-cable system modelled by beam and truss elements, the consistent-mass matrices which can be obtained by the usual finite element procedure⁶⁾ are utilized. It should be noted that the mass of stiffening girders is also added to that of cables. Moreover, the interaction between stiffening girders and cables is not considered in order to simplify the present dynamic analysis.

In order to determine the structural damping properties, the method of modal damping ratios⁶⁾ is chosen in this analysis. By assuming the identical values of modal damping ratios for every vibrational mode of superstructures and substructures of towers, the damping matrix of the tower-cable system including the mass of stiffening girders can be obtained through a free-vibration analysis⁵⁾. The values of modal damping ratios adopted in this study are set to be 2% and 10% for superstructures and substructures, respectively⁴⁾.

3. ANALYTICAL MODELS AND LOADING CONDITIONS

(1) Analytical models

The geometry and cross-section dimensions of the main towers of the Akashi-Kaikyo bridge based on a preliminary design⁷⁾ are given in Ref. 3). As shown in Fig. 1~3, the planar tower model, the planar tower-cable model and the spatial tower-cable model proposed in Ref. 3) are adopted throughout this study. For the dynamic analyses, the substructures of towers, i.e., the pier structures, are added to the bottom of vertical members of towers in order to account for the effects of soil-interaction. As illustrated in Fig. 4, the simple pier model developed in Ref. 8) is employed in the present analysis. By treating this model as the rigid mass with the horizontally translational spring and the rotational spring, the linear stiffness and mass matrices of substructures can be formulated and assembled into those of superstructures⁵⁾.

(2) Loading conditions

Three types of loading conditions are considered in this study as : 1) vertical dead and live loads, 2) horizontal wind loads and 3) horizontal earthquake loads. The first two are treated as static loadings while the last

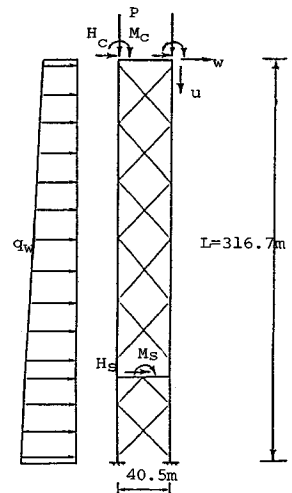


Fig. 1 Planar tower model.

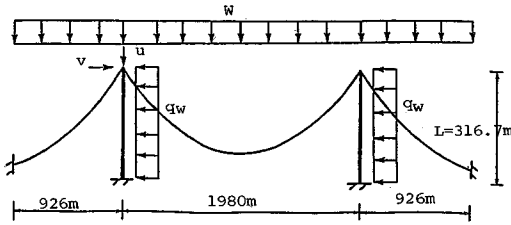


Fig. 2 Planar tower-cable model.

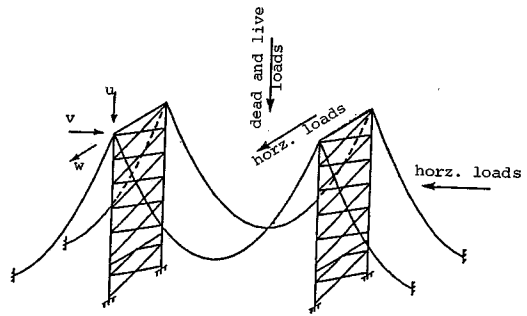


Fig. 3 Spatial tower-cable model.

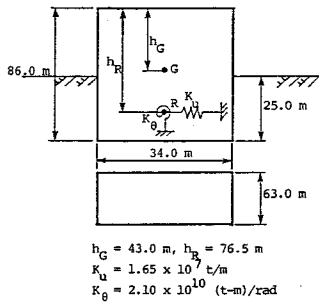


Fig. 4 Pier models of Akashi tower in plane of bridge axis.

Table 1 Additional wind loads.

Node	Type	Loads
14, 15	H_c	3058 (t)
14, 15	M_c	21824 (t-m)
34	H_s	3982 (t)
34	M_s	5973 (t-m)

as dynamic loadings. For the dead and live loads, the full-loading pattern of live loads³⁾ is of primary concern. The uniformly distributed load on cables is denoted by W for the planar and spatial tower-cable models as shown in Fig. 2 and its reaction at the tower top for the planar tower model is P as in Fig. 1. It is noted that the values of design dead and live loads of W , i. e. W_d , are 22.15 t/m for the main span and 22.475 t/m for the side span, respectively, that of P , i. e. P_d , is 50 344 t (t : ton, m : metre)⁷⁾ and those of dead loads of towers⁷⁾ are given in Ref. 3).

a) Static wind loads

The horizontal wind loads acting on the structures in the directions of perpendicular-to-bridge axis and bridge axis as indicated in Fig. 3 are considered in this analysis. The wind loads applied to towers are treated as the uniformly distributed forces per unit projected area against wind, and are denoted by q_w in Fig. 1 and 2. In addition, for wind loads in the perpendicular-to-bridge axis direction, there exist the forces from the cables and the stiffening girders. Due to the distances between the real points where these forces act and the tower nodes, these reactions are treated as the reaction forces and moments, H_c and M_c for the reaction from the cables, and H_s and M_s from the stiffening girders as shown in Fig. 1. For the case of the bridge plane, these reactions from cables and girders, H_c , M_c , H_s and M_s , are excluded¹⁾, since their values are negligible in comparison with the values of wind loads acting on towers. Based on Ref. 7), the design values of q_w are 0.657 t/m² and 0.722 t/m² in the perpendicular plane and bridge plane, respectively, and those of H_c , M_c , H_s , M_s are shown in Table 1. These design wind loads on towers including the above reactions are denoted by q_{wd} for further discussion.

b) Dynamic earthquake loads

Since the accelerogram of the north-south (NS) component of the 1940 El Centro record⁶⁾ is one of the perfect earthquake records⁴⁾, it is selected as the input acceleration \ddot{u}_g in this study. This accelerogram is discretized by the 0.02-second time interval for the 30-second time history and its amplitudes are scaled from those of the real maximum acceleration (=348 gal) in proportion to the design maximum acceleration denoted by a_d (=180 gal) for the purpose of comparison. This design acceleration was obtained by assuming an $M=8$ class earthquake at about 150 km southeast of the construction sites and this earthquake is expected to occur once or twice for every 100-year⁴⁾. In the present study, the input El Centro

accelerogram of maximum acceleration varying from a_d to $4 a_d$ is considered. Based on the statistical data of the past earthquakes in the vicinity of Japanese islands, there exist quite a few number of empirical relationships among the magnitude, the maximum acceleration, the epicentral distance and the seismic wave period⁹⁾. For the same seismic wave as the design earthquake of $M=8$, if the most conservative formula expressing the magnitude to be proportional to the logarithm (base ten) of the maximum amplitude is utilized, the magnitude of earthquake for maximum acceleration equal to $4 a_d$ or 720 gal is approximated to be 8.6 with the epicentral distance about 150 km. This earthquake of $M=8.6$ is unlikely to occur within the life time of structures.

(3) Loading paths

It is very difficult to define the exact loading path to check the safety of structures. However, in order to investigate the structural behaviour, the deterministic loading path must be given. In the present analysis, three representative types of loading paths are defined as follows :

- Loading Path I : keeping the horizontal loads constant and varying the vertical loads,
- Loading Path II : keeping the vertical loads constant and varying the horizontal loads, and
- Loading Path III : varying both horizontal and vertical loads.

In all of these paths the vertical loads mean the dead and live loads of the structures, the horizontal loads mean the wind (or seismic) loads in either the perpendicular plane or the bridge plane. The concept of three loading paths is illustrated in Fig. 5. It is emphasized that the values of either horizontal or vertical loads are varied proportional to those of their respective design loads and a starting point of all paths for the analyses of planar and spatial tower-cable models is chosen to be the state of design dead and live loads as can be seen in Fig. 5⁹⁾.

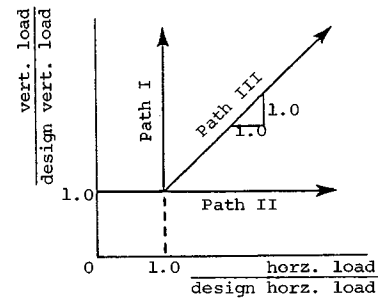


Fig. 5 Loading paths.

4. RESULTS OF STATIC ANALYSES

For the appearance of load-displacement curves, the ratio between loads (P , W or q) and design loads (P_d , W_d or q_d) is plotted against that of the displacement at the tower top (u , v , w) and the tower height (L). The directions of displacement follow those appeared in Fig. 1~3. An ultimate point is represented by a dot on the load-displacement curve.

(1) Load-displacement behaviour

In the case of loading path II, the load-displacement curves for the comparisons of the planar and spatial analyses in the directions of perpendicular-to-bridge axis and bridge axis are shown in Fig. 6 (a) and 6 (b), and in the case of loading path III, they are shown in Fig. 7 (a) and 7 (b), respectively. It is noted that in tracing the curves of spatial tower-cable model as in Fig. 6 the numerical computations become unstable in the vicinity of an ultimate state due to the fact that the spatial tower-cable model in Fig. 3 consists of a huge amount of the number of degree of freedoms (dof), i. e., 630 dof. As can be observed in Fig. 6, 7, the characters of the curves of planar and spatial analyses seem to be alike in the cases of wind loads acting in both directions. Although the load-displacement curves of loading path I are not given here, they also follow a similar trend.

For the comparisons of the ratio between the obtained ultimate loads and the design loads, Table 2 summarizes their values according to three loading paths in the cases of wind loads in the perpendicular-to-bridge axis and bridge axis. It can be seen that for any result of loading paths larger values of the ratio of ultimate loads and design loads are obtained for the spatial analyses compared with the planar analyses in the case of wind loads in the perpendicular-to-bridge axis direction due to the noticeable cable effects improving the performance of the tower behaviour as also found in the case of dead

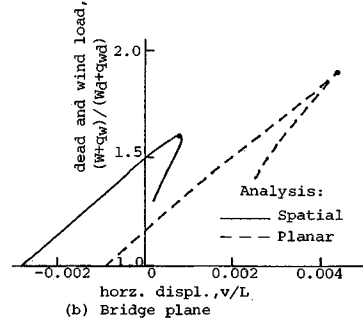
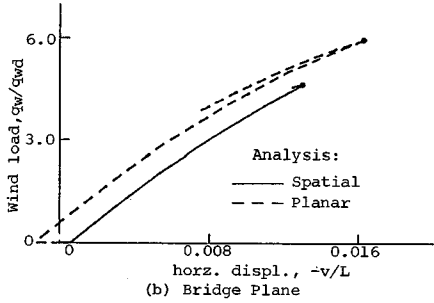
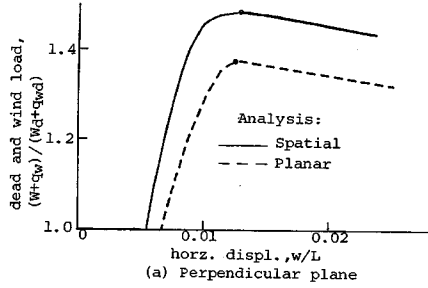
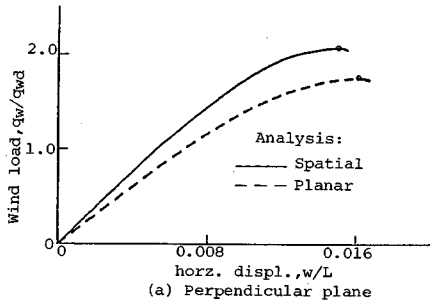


Fig. 6 Load-displacement curves due to loading path II.

Fig. 7 Load-displacement curves due to loading path III.

Table 2 Comparison of ultimate loads for three loading paths.

Loading path	Loading conditions	Planar analysis	Spatial analysis
I (vary only vertical loads)	design wind loads (perpendicular dir.)	1.42	1.90
	design wind loads (bridge dir.)	1.94	1.87
II (vary only horizontal loads)	wind loads (perpendicular dir.)	1.76	2.08
	wind loads (bridge dir.)	6.00	4.60
III (vary both horz. and vert. loads)	wind loads (perpendicular dir.)	1.38	1.48
	wind loads (bridge dir.)	1.90	1.60

and live loads only in Ref. 3). However, the opposite tendency can be observed in the case of wind loads in the bridge axis direction. The reason may be that the behaviour of towers subject to horizontal loadings involves not only an inplane deformation but also an out-of-plane deformation which can not be considered in the case of planar analyses.

(2) Discussions

Regarding to three loading paths considered here, the loading path II involving the increase of horizontal loads and constant vertical loads seems to be the most realistic one. The reason is that the values of design dead and live loads specified in the current codes¹⁾ are close to the maximum loads such that the probability of the design loads being exceeded is very small, while the design wind and earthquake loads are smaller than the measured maximum loads by an economic consideration¹⁰⁾. According to the results of

loading path II in Table 2, the main towers of Akashi-Kaikyo Bridge can resist much larger wind loads in the bridge direction than those in the perpendicular-to-bridge axis direction. The obtained critical values of wind loads in the directions of bridge axis and perpendicular-to-bridge axis are about 4.60 and 2.08 times the specified design wind loads⁷⁾, respectively. Also indicated in Table 2, for the case of loading path III concerned with increasing both horizontal and vertical loads, the ultimate loads of about 1.60 and 1.48 times the design dead, live and wind loads⁷⁾ in the directions of bridge axis and perpendicular-to-bridge axis, respectively, may be a useful information for the future improvements of the design procedure.

From the current code of practice for the design of huge towers of suspension bridges¹⁾ which is based on the allowable stress design concept, the nominal value of factor of safety is implicitly specified to be 1.7 when only the principal loadings, i.e., the dead and live loads are considered. In the case of the combination between the principal loadings and the subsidiary loadings consisting the wind or earthquake loads, the coefficient of increase for allowable stresses being equal to 1.5 is adopted¹⁾. Hence, the specified factor of safety becomes 1.13 (1.7/1.5) when the wind or earthquake loads are included. Since the values of ultimate loads theoretically obtained in this study are nondimensionalized with their design loads specified in the current codes⁷⁾ and since among the three loading paths considered in this study a definition of the loading path III seems to be the most consistent with that of the safety factor 1.13, the ultimate loads obtained based on this loading path III are used for a comparison with the safety factor 1.13. As can be observed from Table 2, larger values of ultimate loads than the expected factor of safety are obtained in the case of the combination of dead, live and wind loads, i.e., $1.48 > 1.13$. The reason for this trend could be the difference due to models and analytical procedures as also indicated in the previous study considering the dead and live loads only in Ref. 3). Therefore, in the design of huge towers of suspension bridges subject to the combination of dead, live and wind loads, more elaborate design procedures, such as the analytical procedures for spatial tower-cable models³⁾, are also encouraged.

5. RESULTS OF DYNAMIC ANALYSES

As discussed previously, the most realistic loading path II is adopted in this chapter. In other words, by keeping the vertical dead and live loads equal to their design values, the nonlinear dynamic analyses of the two planar models, i.e., the planar tower-cable model in Fig. 2 and the planar tower model in Fig. 1, subject to the El Centro accelerogram with variable amplitudes are performed and the results are shown below.

(1) Responses of planar tower-cable model in plane of bridge axis

From the results of free-vibration analyses of the planar tower-cable model including two additional degrees of freedom (horizontal translation and rotation) at the tower bottom per one side of bridge, the vibrations of tower-cable system are governed by cable vibrations from mode no. 1 to 17 and then the towers begin to vibrate from mode no. 18 which corresponds to the natural period of 2.66 sec⁹⁾. By obtaining the free-vibration results of the model without substructures and comparing with those with substructures, it is found that in the range between mode no. 40 and 70 (period between 1.24 sec and 0.14 sec) for the model with substructures, the contributions from substructure vibrations are dominant⁹⁾. It should be noted that since the analysis of tower-cable system is started from the state of design vertical dead and live loads as explained in the chapter 3, the stiffness matrix used in free-vibration analyses involves the effects of axial deformation of structures due to these vertical loads.

a) Responses due to different input acceleration

Fig. 8 shows the responses of relative horizontal displacement of different points along the tower height on one side of the bridge due to the design input acceleration $a_d=180$ gal for the 30-second time history. Although the results on another side of the bridge are not given here, their relative dynamic displacement is observed to be identical to that of the results in Fig. 8. This indicates the in-phase vibrations of the

towers on both sides of the bridge due to the nature of dynamic loadings. It may be of interest to note that the maximum displacement of all nodes except those of node 6, 7 and 8 in Fig. 8 occurs almost simultaneously at time about 6 second.

From the 30-second time history responses of horizontal displacement due to input acceleration with variable amplitudes up to $4 a_d$, almost the same wave form as that in Fig. 8 with different magnitudes are observed for all cases of variable input acceleration. Fig. 9 (a) shows the distribution of maximum relative horizontal displacement along the tower height for the different input acceleration. The comparisons of magnitudes of maximum internal stress resultants inside the tower cross-section are given in Fig. 9 (b) for the bending moment and in Fig. 9 (c) for the axial compression. The resistance of tower cross-section, i. e., a yield moment and a yield force, are also shown in both figures. To examine whether the tower cross-section yields under the earthquake excitation, the following yielding criteria is adopted in this study as

$$f(N_m, M_m) = \frac{N_m}{N_y} + \frac{M_m}{M_y} = 1.0 \dots\dots\dots (5)$$

where N_m and M_m denote the magnitudes of maximum axial compression and bending moment at the particular time when $f(N_m, M_m)$ becomes maximum, and N_y and M_y denote the yield force and moment, respectively. Even for the case of input acceleration equal to $4 a_d$, the maximum value of $f(N_m, M_m)$ taking place at the cross-section about one-fourth of tower height from the tower top is approximately equal to 0.97 less than 1.0. This critical cross-section corresponds to the point where the material property is changed from higher strength to lower one as can be observed from the distribution of either resisting yield moment in Fig. 9 (b) or resisting yield force in Fig. 9 (c). Consequently, the tower does not undergo complete yielding for the horizontal ground acceleration up to 4 times the design acceleration in the plane of bridge axis.

It should be also noted that the time when the maximum stress resultants occur is less than 10 second despite some peaks of input acceleration existing beyond 10-second time history⁵⁾. This may be explained by negligible effects of inelasticities on the tower responses.

b) Effects of substructures on tower behaviour

Up to this stage, all of the results in this section are obtained by including the substructures at the tower bottom. In order to investigate influences of the substructures on the dynamic behaviour of towers, the analyses of the planar tower-cable model without substructures are performed in case of design input acceleration a_d . Fig. 10 (a) and 10 (b) indicate the magnitudes of maximum relative displacement and those

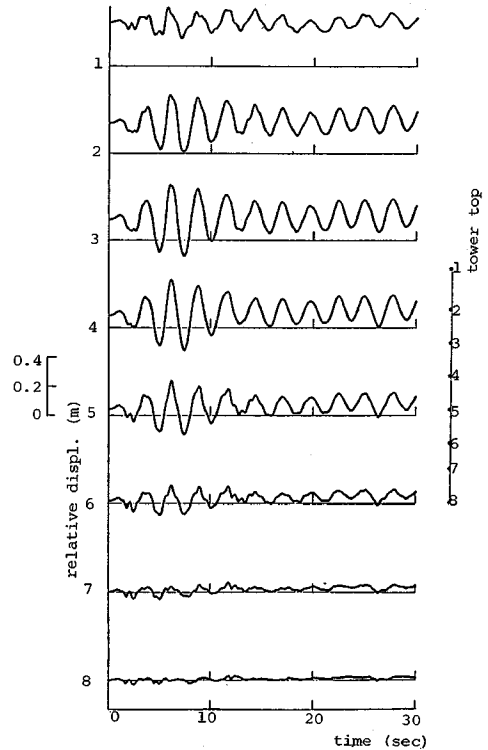


Fig. 8 Relative horizontal displacement responses of planar tower-cable model due to input a_d .

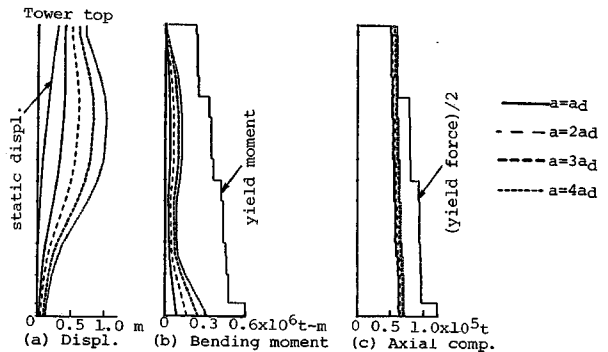


Fig. 9 Comparison of magnitude of maximum responses of planar tower-cable model.

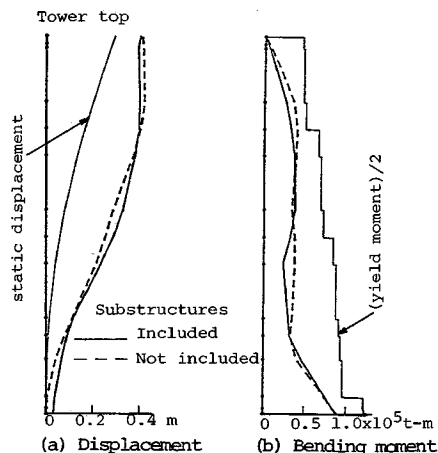


Fig. 10 Comparison of magnitude of maximum responses due to effects of substructures.

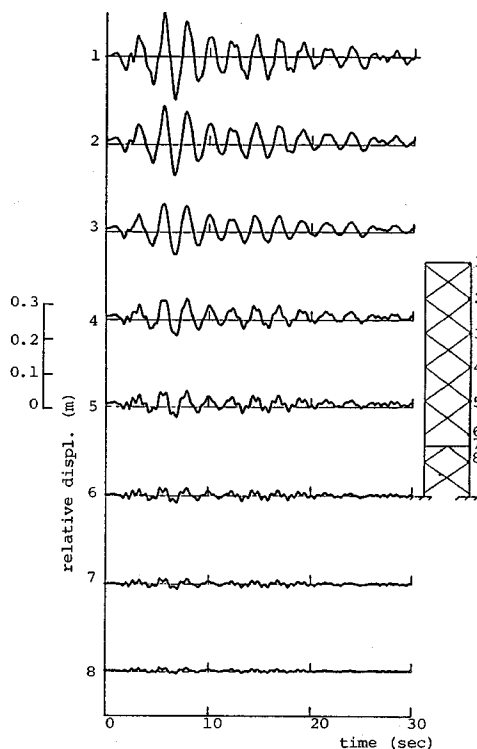


Fig. 11 Relative horizontal displacement responses of planar tower model due to input a_d .

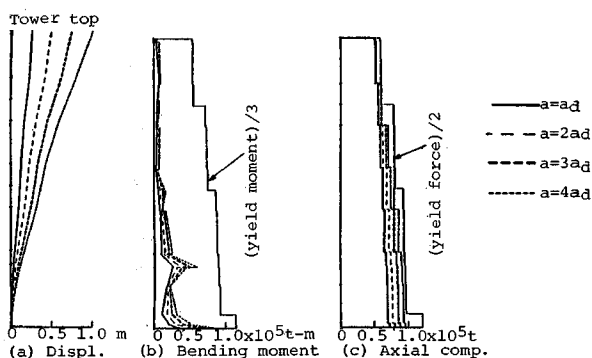


Fig. 12 Comparison of magnitude of maximum responses of planar tower model.

of maximum bending moment, respectively. Allowing the horizontal translation and rotation at the bottom of towers, the system with substructures naturally exhibits larger displacement responses as illustrated in Fig. 10 (a). On the contrary, Fig. 10 (b) shows that the maximum bending moment arising inside tower cross-section for the case without substructures seems to be larger. Hence, neglecting effects of substructures seems to give more conservative results. In the following analyses of the planar tower model in plane of perpendicular-to-bridge axis, the substructures are excluded by this reason.

(2) Responses of planar tower model in plane of perpendicular-to-bridge axis

For the results of free-vibration analyses in this case, the natural period of the lowest mode of the planar tower model in Fig. 1 is about 2.27 second.

In the case of input acceleration equal to a_d for the 30-second period, Fig. 11 indicates the responses of relative horizontal displacement of different points of one leg of vertical tower members. Differing from the above results of the planar tower-cable model in Fig. 8, much less horizontal displacement due to static design dead and live loads than the dynamic displacement can be observed in Fig. 11. This may be because the effects of cables are neglected in the analyses of the planar tower model. It is noted that the time when the maximum displacement of all tower nodes occurs is ranging between 5 and 8 second.

Similar to the case of the planar-tower model, almost identical wave forms of displacement responses for variable input acceleration up to $4 a_d$ are observed in this case of the planar tower model. Fig. 12 (a), 12 (b) and 12 (c) illustrate the comparisons of magnitudes of maximum relative displacement, bending moment

and axial compression, respectively, in which only their distribution along the vertical members of towers is plotted. In order to examine yielding of towers, the maximum value of $f (M_m, N_m)$ in Eq. (5) is calculated to be about 0.70 for the input $4 \alpha_d$. The critical cross-section is located around one-fourth of tower height from the tower bottom where a horizontal bracing member is connected to the vertical members (see node no. 7 in Fig. 11). It is noted that the time of occurrence of maximum stress resultant is also less than 10 second. Moreover, the level of stress resultants at the critical cross-section of bracing members is checked to be lower than that of vertical members during the strong earthquake excitation.

From the above results of the planar analyses of towers of Akashi-Kaikyo Bridges in the bridge and perpendicular-to-bridge axis directions, the towers can resist elastically against the 1940 El Centro accelerogram with maximum acceleration of 4 times the design ground acceleration in both directions. Nevertheless, it is emphasized that these conclusions are drawn under the assumption that the failure of the substructures of towers, i. e., the pier structures, due to yielding is not taken into consideration in this analysis.

6. CONCLUSIONS

The following conclusions have been drawn from this study.

(1) The combined tower-cable model and the analytical procedures for the tower-cable model as proposed in the previous work³⁾ can be adopted successfully to obtain both nonlinear static and dynamic responses of the main towers of long-span suspension bridges subjected to a variety of the combinations of the vertical dead and live loads, and the horizontal wind or earthquake loads.

(2) From the results of ultimate strength analyses of the main towers of the Akashi-Kaikyo Bridge under the combinations of the vertical dead and live loads, and the horizontal wind loads which are based on three loading path considered in this analysis, the ratio between the obtained ultimate strength and the design loads for the case of loading path III, i. e., varying all combined loads, is about 1.48 which is larger than the specified factor of safety of 1.13. According to the results of the most realistic loading path II, in which the design dead and live loads are kept constant, the obtained critical values of wind loads in the directions of perpendicular-to-bridge axis and bridge axis are about 2.08 and 4.60 times the design wind loads, respectively.

(3) Under the applications of the design vertical dead and live loads, and the horizontal ground motions of the north-south component of 1940 El Centro accelerogram with variable amplitudes, the Akashi towers are safe as much as 4 times the design earthquake acceleration by an elastic resistance without any serious yielding. This acceleration for which the structures can resist elastically corresponds to rather strong earthquake with the magnitude of approximately 8.6 with the epicentral distance about 150 km. It is emphasized that the planar behaviour of the superstructures of towers against this strong earthquake is of primary concern in this study. It is also noted that the above conclusion has been obtained under the assumption that the present dynamic analysis does not consider the interaction between stiffening girders and cables. The effect of the interaction remains to be clarified through future study.

(4) Due to the difference in the ultimate strength for the static results of spatial and planar analyses, in the design of huge structures, such as the towers of Akashi-Kaikyo Bridge, subject to the combinations of the vertical and horizontal loads, more elaborate design procedures incorporating spatial behaviour of tower-cable system are preferred as a matter of accurate and economic design.

7. ACKNOWLEDGEMENTS

This paper is based on the doctoral dissertation of the first author at the University of Tokyo, who was awarded the scholarship by the Japanese Government. The work is also supported by the research grant through the Honshu-Shikoku Bridge Authority. The authors are indebted to Dr. Hideyuki Horii, Dr. Yozo Fujino and Dr. Pacheco Benito of the University of Tokyo for their valuable suggestions.

REFERENCES

- 1) Honshu-Shikoku Bridge Authority : Guideline for the Design of Main Towers, 1980 (in Japanese).
- 2) Honshu-Shikoku Bridge Authority : Outline of Honshu-Shikoku Bridge Project, 1983.
- 3) Chaisomphob, T., Hasegawa, A. and Nishino, F. : A Static Nonlinear Behaviour of Steel Towers of Long-Span Suspension Bridges Subject to Dead and Live Loads, Proc. of JSCE, Structural Engineering/Earthquake Engineering, Vol. 5, No. 2, pp. 225 s-233 s, October 1988 (Proc. of JSCE No. 398/ I -10).
- 4) Honshu-Shikoku Bridge Authority : Specifications for Earthquake-Resistant Design, 1977 (in Japanese).
- 5) Chaisomphob, T. : The Inelastic Finite Displacement Behaviour of Steel Towers of Long-Span Suspension Bridges, thesis presented to Univ. of Tokyo, in 1987, in partial fulfillment of the requirements for the degree of Doctor of Engineering.
- 6) Clough, R.W. and Penzien, J. : Dynamics of Structures, McGraw-Hill, 1982.
- 7) Honshu-Shikoku Bridge Authority : A Preliminary Design of the Akashi-Kaikyo Bridge, Unpublished document (in Japanese).
- 8) Honshu-Shikoku Bridge Authority : A Report on Earthquake Resistance of Substructures of Honshu-Shikoku Bridge, 1985 (in Japanese).
- 9) Japan Society of Civil Engineerings : Handbook of Vibrations for Civil Engineers, 2nd Ed., 1985 (in Japanese).
- 10) Nishino, F., Sato, N. and Hasegawa, A. : Critical Comments on the Recent Trends of Design Code Changes to Load Factor Design, Proc. Japan-Thai Civil Engrg. Conf., Bangkok, Mar. 1985.

(Received November 7 1988)
